N2N Learning: Network to Network Compression via Policy Gradient Reinforcement Learning

Anubhav Ashok
Robotics Institute
Carnegie Mellon University
bhav@cmu.edu

Nicholas Rhinehart
Robotics Institute
Carnegie Mellon University
nrhineha@cs.cmu.edu

Fares Beainy
Volvo Construction Equipment
fares.beainy@volvo.com

Kris M. Kitani
Robotics Institute
Carnegie Mellon University
kkitani@cs.cmu.edu

Abstract

While bigger and deeper neural network architectures continue to advance the state-of-the-art for many computer vision tasks, real-world adoption of these networks is impeded by hardware and speed constraints. Conventional model compression methods attempt to address this problem by modifying the architecture manually or using pre-defined heuristics. Since the space of all reduced architectures is very large, modifying the architecture of a deep neural network in this way is a difficult task. In this paper, we tackle this issue by introducing a principled method for *learning* reduced network architectures in a data-driven way using reinforcement learning. Our approach takes a larger 'teacher' network as input and outputs a compressed 'student' network derived from the 'teacher' network. In the first stage of our method, a recurrent policy network aggressively removes layers from the large 'teacher' model. In the second stage, another recurrent policy network carefully reduces the size of each remaining layer. The resulting network is then evaluated to obtain a reward – a score based on the accuracy and compression of the network. Our approach uses this reward signal with policy gradients to train the policies to find a locally optimal student network. Our experiments show that we can achieve compression rates of more than $10\times$ for models such as ResNet-34 while maintaining similar performance to the input 'teacher' network. We also present a valuable transfer learning result which shows that policies which are pre-trained on smaller 'teacher' networks can be used to rapidly speed up training on larger 'teacher' networks.

1 Introduction

While carefully hand-designed deep convolutional networks continue to increase in size and in performance, they also require significant power, memory and computational resources, often to the point of prohibiting their deployment on smaller devices. As a result, researchers have developed model compression techniques based on Knowledge Distillation to compress a large (teacher) network to a smaller (student) network using various training techniques (e.g., soft output matching, hint layer matching, uncertainty modeling). Unfortunately, state-of-the-art knowledge distillation methods share a common feature: they require carefully *hand-designed* architectures for the student model. Hand-designing networks is a tedious sequential process, often loosely guided by a sequence of trial-and-error based decisions to identify a smaller network architecture. This process makes it very difficult to know if the resulting network is optimal. Clearly, there is a need to develop more principled methods of identifying optimal student architectures.

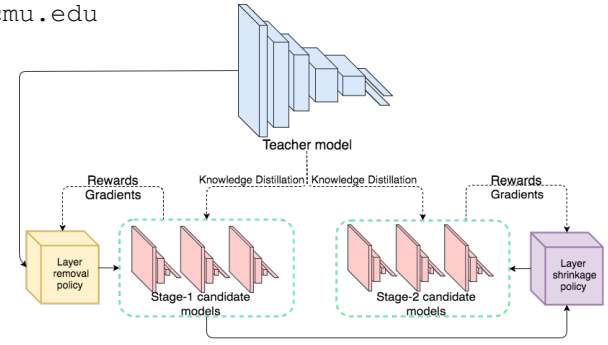

Figure 1: Layer Removal Policy removes layers of Teacher network architecture (stage-1 candidates) then Layer Shrinkage Policy reduces parameters (stage-2 candidates).

Towards a more principled approach to network architecture compression, we present a reinforcement learning approach to *identify a compressed high-performance architecture (student) given knowledge distilled from a larger high-performing model (teacher)*. We make a key conceptual assumption that formulates the sequential process of converting a teacher network to a student network as a Markov Decision Process (MDP). Under this model, a state s represents the network architecture. Clearly, the domain of the state $\mathcal{S}$ is very large since it contains every possible reduced architecture of the teacher network. A deterministic transition in this state space, $T(s'|s,a)$, is determined by selecting the action a, e.g., removing a convolutional filter or reducing the size of a fully connected layer. Each action will transform one architecture s to another architecture s'. Under the MDP, the strategy for selecting an action given a certain state is represented by the policy $\pi(a|s)$, which stochastically maps a state to an action. The process of reinforcement learning is used to learn an optimal policy based on a reward function $r(s)$ defined over the state space. In our work, we define the reward function based on the *accuracy* and the *compression*

rate of the specified architecture s.

A straightforward application of reinforcement learning to this problem can be very slow depending on the definition of the action space. For example, an action could be defined as removing a single filter from every layer of a convolutional neural network. Since the search space is exponential in the size of the action space and sequence length, it certainly does not scale to modern networks that have hundreds of layers.

Our proposed approach addresses the problem of scalability in part, by introducing a two-stage action selection mechanism which first selects a macro-scale "layer removal" action, followed by a micro-scale "layer shrinkage" action. In this way we enable our reinforcement learning process to efficiently explore the space of reduced networks. Each network architecture that is generated by our policy is then are trained with Knowledge Distillation (Hinton, Vinyals, and Dean 2015). Figure 1 illustrates our proposed approach.

To the best of our knowledge, this is the first paper to provide a principled approach to the task of network compression, where the architecture of the student network is obtained via reinforcement learning. To facilitate reinforcement learning, we propose a reward function that encodes both the compression rate and the accuracy of the student model. In particular, we propose a novel formulation of the compression reward term based on a relaxation of a constrained optimization problem, which encodes the hardware-based computational budget items in the form of linear constraints.

We demonstrate the effectiveness of our approach over several network architectures and several visual learning tasks of varying difficulty (MNIST, SVHN, CIFAR-10, CIFAR-100, Caltech-256). We also demonstrate that the compression policies exhibit generalization across networks with similar architectures. In particular, we use a policy trained on a ResNet-18 model on a ResNet-34 model and show that it greatly accelerates the reinforcement learning process.

2 Related Work

We first discuss methods for compressing models to a manually designed network (pruning and distillation). Towards automation, we discuss methods for automatically constructing high-performance networks, orthogonal to the task of compression.

Pruning: Pruning-based methods preserve the weights that matter most and remove the redundant weights (LeCun et al. 1989), (Hassibi, Stork, and Wolff 1993), (Srinivas and Babu 2015), (Han et al. 2015), (Han, Mao, and Dally 2015), (Mariet and Sra 2015), (Anwar, Hwang, and Sung 2015), (Guo, Yao, and Chen 2016). While pruning-based approaches typically operate on the weights of the teacher model, our approach operates on a much larger search space over both model weights and model architecture. Additionally, our method offers greater flexibility as it allows the enforcement of memory, inference time, power, or other hardware constraints. This allows our approach to find the optimal architecture for the given dataset and constraints instead of being limited to that of the original model.

Knowledge Distillation: Knowledge distillation is the task of training a smaller network (a "student") to mimic a "teacher" network, performing comparably to the input network (a "teacher") (Bucilu, Caruana, and Niculescu-Mizil 2006), (Ba and Caruana 2014), (Hinton, Vinyals, and Dean 2015), (Romero et al. 2014), (Urban et al. 2016). The work of (Hinton, Vinyals, and Dean 2015) generalized this idea by training the student to learn from both the teacher and from the training data, demonstrating that this approach outperforms models trained using only training data. In (Romero et al. 2014), the approach uses Knowledge Distillation with an intermediate hint layer to train a thinner but deeper student network containing fewer parameters to outperform the teacher network. In previous Knowledge Distillation approaches, the networks are hand designed, possibly after many rounds of trial-and-error. In this paper, we train a policy to learn the optimal student architecture, instead of hand-designing one. In a sense, we *automate Knowledge Distillation*, employing the distillation method of (Ba and Caruana 2014) as a component of our learning process. In the experiments section we show that our learned architectures outperform those described in (Romero et al. 2014) and (Hinton, Vinyals, and Dean 2015).

Architecture Search: There has been much work on exploring the design space of neural networks (Saxe et al. 2011), (Zoph and Le 2016), (Baker et al. 2016), (Ludermir, Yamazaki, and Zanchettin 2006), (Miikkulainen et al. 2017), (Real et al. 2017), (Snoek, Larochelle, and Adams 2012), (Snoek et al. 2015), (Stanley and Miikkulainen 2002), (Jozefowicz, Zaremba, and Sutskever 2015), (Murdock et al. 2016), (Feng and Darrell 2015), (Warde-Farley, Rabinovich, and Anguelov 2014), (Iandola et al. 2016). The principal aim of previous work in architecture search has been to build models that maximize performance on a given dataset. On the other hand, our goal is to find a compressed architecture while maintaining reasonable performance on a given dataset. Our approach also differs from existing architecture search method since we use the teacher model as the search space for our architecture instead of constructing networks from scratch. Current methods that construct networks from scratch either operate on a very large search space, making it computationally expensive (Zoph and Le 2016), (Real et al. 2017), (Miikkulainen et al. 2017), (Jozefowicz, Zaremba, and Sutskever 2015) or operate on a highly restricted search space (Baker et al. 2016), (Snoek et al. 2015). Our approach instead leverages the idea that since the teacher model is able to achieve high accuracy on the dataset, it already contains the components required to solve the task well and therefore is a suitable search space for the compressed architecture.

3 Approach

Our goal is to learn an optimal compression strategy (policy) via reinforcement learning, that takes a Teacher network as

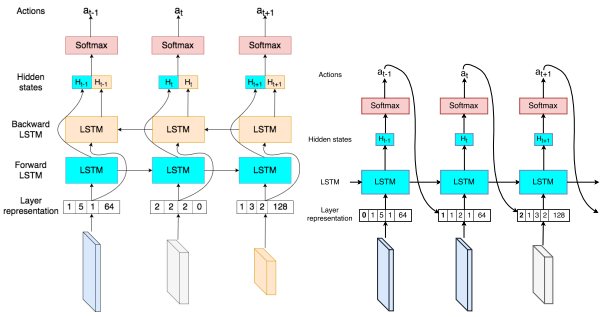

(a) (b)

Figure 2: **a)** Layer removal policy network, **b)** Layer shrinkage policy network

input and systematically reduces it to output a small Student network.

3.1 Markov Decision Process

We formulate the sequential process of finding a reduced architecture as a sequential decision making problem. The decision process is modeled as a Markov Decision Process (MDP). Formally, the MDP is defined as the tuple $\mathcal{M} = \{\mathcal{S}, \mathcal{A}, T, r, \gamma\}$.

States: $\mathcal{S}$ is the state space, a finite set consisting of all possible reduced network architectures that can be derived from the Teacher model. For example, a VGG network (Simonyan and Zisserman 2014) represents the state $s \in \mathcal{S}$ (the initial state) and by removing one convolutional filter from the first layer we obtain a new network architecture s'.

Actions: $\mathcal{A}$ is a finite set of actions that can transform one network architecture into another network architecture. In our approach there are two classes of action types: layer removal actions and layer parameter reduction actions. The definition of these actions are further described in Section 3.2 and 3.2.

Transition Function: $T : \mathcal{S} \times \mathcal{A} \to \mathcal{S}$ is the state transition dynamic. Here, T is deterministic since an action a always transforms a network architecture s to the resulting network architecture s' with probability one.

Discount Factor: γ is the discount factor. We use $\gamma = 1$ so that all rewards contribute equally to the final return.

Reward: $r : \mathcal{S} \to \mathbb{R}$ is the reward function. The rewards of network architecture $r(s)$ can be interpreted to be a score associated with a given network architecture s. Note that we define the reward to be 0 for intermediate states, which represent "incomplete" networks, and only compute a non-trivial reward for the final state. The reward function is described in detail in Section 3.4.

3.2 Student-Teacher Reinforcement Learning

Under this MDP, the task of reinforcement learning is to learn an optimal policy $\pi : \mathcal{S} \to \mathcal{A}$, such that it maximizes the expected total reward, with the total reward given by:

$$R(\vec{s}) = \sum_{i=0}^{L=|\vec{s}|} r(s_i) = r(s_L). \quad (1)$$

We take a policy gradient reinforcement learning approach and iteratively update the policy based on sampled estimates of the reward. The design of the action space is critical for allowing the policy gradient method to effectively search the state space. If the actions are selected to be very incremental, a long sequence of actions would be needed to make a significant change to the network architecture, making credit assignment difficult. To address this issue, we propose a two stage reinforcement learning procedure. In the first stage a policy selects a sequence of actions deciding whether to keep or remove each layer of the teacher architecture. In the second stage, a different policy selects a sequence of discrete actions corresponding to the magnitude by which to attenuate configuration variables of each remaining layer. In this way, we are able to efficiently explore the state space to find the optimal student network.

Algorithm 1 Student-Teacher Reinforcement Learning

procedure STUDENT-TEACHER RL($\mathcal{S}, \mathcal{A}, T, r, \gamma$)
  $s_0 \leftarrow$ Teacher
  for $i = 1$ to N_1 **do** ▷ Layer removal
    for $t = 1$ to L_1 **do**
      $a_t \sim \pi_{\text{remove}}(s_{t-1}; \theta_{\text{remove},i-1})$
      $s_t \leftarrow T(s_{t-1}, a_t)$
    end for
    $R \leftarrow r(s_{L_1})$
    $\theta_{\text{remove},i} \leftarrow \nabla_{\theta_{\text{remove},i-1}} J(\theta_{\text{remove},i-1})$ ▷ (Eq. 2)
  end for
  $s_0 \leftarrow$ Stage-1 Candidate
  for $i = 1$ to N_2 **do** ▷ Layer shrinkage
    for $t = 1$ to L_2 **do**
      $a_t \sim \pi_{\text{shrink}}(s_{t-1}; \theta_{\text{shrink},i-1})$
      $s_t \leftarrow T(s_{t-1}, a_t)$
    end for
    $R \leftarrow r(s_{L_2})$
    $\theta_{\text{shrink},i} \leftarrow \nabla_{\theta_{\text{shrink},i-1}} J(\theta_{\text{shrink},i-1})$ ▷ (Eq. 2)
  end for
  Output: Compressed model
end procedure

A sketch of the algorithm is given in Algorithm 3.2. For both layer removal and shrinkage policies, we repeatedly sample architectures and update the policies based on the reward achieved by the architectures. We now describe the details of the two stages of student-teacher reinforcement learning.

Layer removal In the layer removal stage, actions a_t correspond to the binary decision to keep or remove a layer. The length of the trajectory for layer removal is $T = L$, the number of layers in the network. At each step t of layer removal, the Bidirectional LSTM policy (See Figure 2a) observes the hidden states, h_{t-1}, h_{t+1}, as well as information x_t about the current layer: $\pi_{\text{remove}}(a_t | h_{t-1}, h_{t+1}, x_t)$. Information about the current layer l is given as

$$x_t = (l, k, s, p, n, s_{\text{start}}, s_{\text{end}}),$$

where l is the layer type, k kernel size, s stride, p padding and n number of outputs (filters or connections). To model more complex architectures, such as ResNet, s_{start} and s_{end} are used to inform the policy network about skip connections. For a layer inside a block containing a skip connection, s_{start} is the number of layers prior to which the skip connection began and s_{end} is the number of layers remaining until the end of the block. Additionally it is to be noted that although actions are stochastically sampled from the outputs at each time step, the hidden states that are passed on serve as a sufficient statistic for $x_0, a_0 ... x_{t-1}, a_{t-1}$(Wierstra et al. 2010).

Layer shrinkage The length of the trajectory for layer shrinkage is $T = \sum_{l=1}^{L} H_l$, where H is the number of configuration variables for each layer. At each step t of layer shrinkage, the policy observes the hidden state h_{t-1}, the previously sampled action a_{t-1} and current layer information x_t: $\pi_{\text{shrink}}(a_t|a_{t-1}, h_{t-1}, x_t)$. The parameterization of x_t is similar to layer removal except that the previous action is appended to the representation in an autoregressive manner (See Figure 2b). The action space for layer shrinkage is defined as $a_t \in [0.1, 0.2, \ldots, 1]$ (each action corresponds to how much to shrink a layer parameter) and an action is produced for each configurable variable for each layer. Examples include kernel size, padding, and number of output filters or connections.

3.3 Reward function

We define a joint objective function consisting of two components - accuracy and compression, both of which we intend to maximize in student models. We define the reward as follows:

$$R = R_c \cdot R_a$$

Where $R_c \in [0, 1]$ and $R_a \in [0, 1]$ refer to the compression and accuracy reward respectively. R_c is computed using a non-linear function that biases the policy towards producing models with higher compression. It is defined as $R_c = C(2-C)$. The relative compression is defined in terms of the ratio of trainable parameters of each model: $C = 1 - \frac{\#\text{params(student)}}{\#\text{params(teacher)}}$, We define our reward for accuracy, R_a, with respect to the teacher model as $R_a = \min(\frac{A}{A_{\text{teacher}}}, 1)$, where A refers to the accuracy obtained by the student model after being trained for 5 epochs and A_{teacher} refers to the accuracy obtained by the teacher model. We threshold the reward at 1 since we do not want to reward the policy for producing large models which exceed A_{teacher}. Since the rewards are normalized with respect to the teacher, they generalize across tasks and do not require task-specific weighting. Finally, a reward of -1 is assigned to degenerate architectures (larger than parent, null architecture, etc.)

Constraints as Rewards Our approach allows us to incorporate pre-defined hardware or resource budget constraints by rewarding architectures that meet the constraints and discouraging those that do not. Formally, our constrained optimization problem is

$$\begin{aligned} &\max E_{a_{1:T}}[R] \\ &\text{subject to } Ax \leq b, \end{aligned}$$

where A and b form our constraints, and x is vector of constrained variables. We relax these hard constraints by redefining our reward function as:

$$R = \begin{cases} R_a \cdot R_c & \text{if } Ax \leq b \\ -1 & \text{otherwise.} \end{cases}$$

The introduction of the non-smooth penalty may result in a reduced exploration of the search space and hence convergence to a worse local minimum. To encourage early exploration gradually incorporate constraints over time:

$$R = \begin{cases} R_a \cdot R_c & \text{if } Ax \leq b \\ \epsilon_t(R_a \cdot R_c + 1) - 1 & \text{otherwise,} \end{cases}$$

where $\epsilon_t \in [0, 1]$ monotonically decreases with t and $\epsilon_0 = 1$. As it is possible to incorporate a variety of constraints such as memory, time, power, accuracy, label-wise accuracy, our method is flexible enough to produce models practically viable in a diversity of settings. This is in contrast to conventional model compression techniques which require many manual repetitions of the algorithm in order to find networks that meet the constraints as well as optimally balance the accuracy-size tradeoff.

3.4 Optimization

We now describe the optimization procedure for each our stochastic policies, π_{remove} and π_{shrink}. The procedure is the same for each policy, thus we use π in what follows. Each policy network is parameterized by its own θ.

Our objective function is the expected reward over all sequences of actions $a_{1:T}$, i.e.:

$$J(\theta) = E_{a_{1:T} \sim P_\theta}(R)$$

We use the REINFORCE policy gradient algorithm from Williams (Williams 1992) to train both of our policy networks.

$$\begin{aligned} \nabla_\theta J(\theta) &= \nabla_\theta E_{a_{1:T} \sim P_\theta}(R) \\ &= \sum_{t=1}^{T} E_{a_{1:T} \sim P_\theta}[\nabla_\theta \log P_\theta(a_t|a_{1:(t-1)})R] \\ &\approx \frac{1}{m} \sum_{k=1}^{m} \sum_{t=1}^{T} [\nabla_\theta \log P_\theta(a_t|h_t)R_k] \end{aligned}$$

where m is the number of rollouts for a single gradient update, T is the length of the trajectory, $P_\theta(a_t|h_t)$ is the probability of selecting action a_t given the hidden state h_t, generated by the current stochastic policy parameterized by θ and R_k is the reward of the k^{th} rollout.

The above is an unbiased estimate of our gradient, but has high variance. A common trick is to use a state-independent baseline function to reduce the variance:

$$\nabla_\theta J(\theta) \approx \frac{1}{m} \sum_{k=1}^{m} \sum_{t=1}^{T} [\nabla_\theta \log P_\theta(a_t|h_t)(R_k - b)] \qquad (2)$$

We use an exponential moving average of the previous rewards as the baseline b. An Actor-Critic policy was also tested. While there was a minor improvement in stability, it failed to explore as effectively in some cases, resulting in a locally optimal solution. Details are in the supplemental material.

3.5 Knowledge distillation

Student models are trained using data labelled by a teacher model. Instead of using hard labels, we use the unnormalized log probability values (the logits) of the teacher model. Training using the logits helps to incorporate *dark knowledge* (Hinton, Vinyals, and Dean 2015) that regularizes students by placing emphasis on the relationships learned by the teacher model across all of the outputs.

As in (Ba and Caruana 2014), the student is trained to minimize the mean L_2 loss on the training data $\left\{(x^i, z^i)\right\}_{i=1}^{N}$. Where z^i are the logits of the teacher model.

$$\mathcal{L}_{\text{KD}}(f(x;W),z) = \frac{1}{N}\sum_i ||f(x^{(i)};W) - z^{(i)}||_2^2$$

where W represents the weights of the student network and $f(x^{(i)};W)$ is the model prediction on the i^{th} training data sample.

Final student models were trained to convergence with hard and soft labels using the following loss function.

$$\mathcal{L}(\mathcal{W}) = \mathcal{L}_{\text{hard}}(f(x;W),y_{\text{true}}) + \lambda * \mathcal{L}_{\text{KD}}(f(x;W),z)$$

Where $\mathcal{L}_{\text{hard}}$ is the loss function used for training with hard labels (in our case cross-entropy) and y_{true} are the ground truth labels.

4 Experiments

In the following experiments, we first show that our method is able to find highly compressed student architectures with high performance on multiple datasets and teacher architectures, often exceeding performance of the teacher model. Then we demonstrate the viability of our method in highly resource constrained conditions by running experiments with strong model size constraints. Finally, we show that it is possible to rapidly speed up training when using larger teacher models by reusing policies that are pretrained on smaller teacher models.

4.1 Datasets

MNIST The MNIST (LeCun, Cortes, and Burges 1998) dataset consists of 28×28 pixel grey-scale images depicting handwritten digits. We use the standard 60,000 training images and 10,000 test images for experiments. Although MNIST is easily solved with smaller networks, we used a high capacity models (e.g., VGG-13) to show that the policies learned by our approach are able to effectively and aggressively remove redundancies from large network architectures.

Table 1: Summary of Compression results.

Architecture		Acc.	#Params	Δ Acc.	Compr.
MNIST					
VGG-13	Teacher	99.54%	9.4M	—	—
	Student (Stage1)	99.55%	73K	0.01%	127x
CIFAR-10					
VGG-19	Teacher	91.97%	20.2M	—	—
	Student (Stage1)	92.05%	1.7M	+0.08%	11.8x
	Student (Stage1+Stage2)	91.64%	984K	-0.33%	20.53x
ResNet-18	Teacher	92.01%	11.17M	—	—
	Student (Stage1)	91.97%	2.12M	-0.04%	5.26x
	Student (Stage1+Stage2)	91.81%	1.00M	-0.2%	11.10x
ResNet-34	Teacher	92.05%	21.28M	—	—
	Student (Stage1)	93.54%	3.87M	+1.49%	5.5x
	Student (Stage1+Stage2)	92.35%	2.07M	+0.30%	10.2x
SVHN					
ResNet-18	Teacher	95.24%	11.17M	—	—
	Student (Stage1)	95.66%	2.24M	+0.42%	4.97x
	Student (Stage1+Stage2)	95.38%	564K	+0.18%	19.8x
CIFAR-100					
ResNet-18	Teacher	72.22%	11.22M	—	—
	Student (Stage1)	69.64%	4.76M	-2.58%	2.35x
	Student (Stage1+Stage2)	68.01%	2.42M	-4.21%	4.64x
ResNet-34	Teacher	72.86%	21.33M	—	—
	Student (Stage1)	70.11%	4.25M	-2.75%	5.02x
Caltech256					
ResNet-18	Teacher	47.65%	11.31M	—	—
	Student (Stage1)	44.71%	3.62M	-2.94%	3.12x

CIFAR-10 The CIFAR-10 (Krizhevsky and Hinton 2009) dataset consists of 10 classes of objects and is divided into 50,000 train and 10,000 test images (32x32 pixels). This dataset provides an incremental level of difficulty over the MNIST dataset, using multi-channel inputs to perform model compression.

SVHN The Street View House Numbers (Netzer et al. 2011) dataset contains 3232 colored digit images with 73257 digits for training, 26032 digits for testing. This dataset is slightly larger that CIFAR-10 and allows us to observe the performance on a wider breadth of visual tasks.

CIFAR-100 To further test the robustness of our approach, we evaluated it on the CIFAR-100 dataset. CIFAR-100 is a harder dataset with 100 classes instead of 10, but the same amount of data, 50,000 train and 10,000 test images (32x32). Since there is less data per class, there is a steeper size-accuracy tradeoff. We show that our approach is able to produce solid results despite these limitations.

Caltech-256 To test the effectiveness of our approach in circumstances where data is *sparse*, we run experiments on the Caltech-256 dataset (Griffin, Holub, and Perona 2007). This dataset contains more classes and less data per class than CIFAR-100, containing 256 classes and a total of 30607 images (224x224). We trained the networks from scratch instead of using pretraining in order to standardize our comparisons across datasets.

4.2 Training details

In the following experiments, student models were trained as described in Section 3.5. We observed heuristically that 5

epochs was sufficient to compare performance.

The layer removal and layer shrinkage policy networks were trained using the Adam optimizer with a learning rate of 0.003 and 0.01 respectively. Both recurrent policy networks were trained using the REINFORCE algorithm (batch size=5) with standard backpropagation through time. A grid search was done to determine the ideal learning rate and batch size (details in supplemental material).

4.3 Compression Experiments

In this section we evaluate the ability of our approach to learn policies to find compressed architectures without any constraints. In the following experiments, we expect that the policies learned by our approach will initially start out as random and eventually tend towards an optimal size-accuracy trade-off which results in a higher reward. Definitions of architectures are available in the supplemental material.

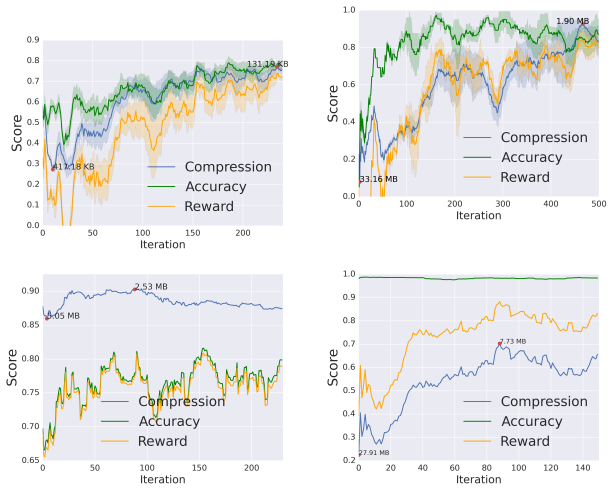

(a) CONV4 (b) VGG-13

Figure 3: Student learning on **MNIST**. Reward, Accuracy, Compression vs Iteration (**Top**: Stage 1, **Bottom**: Stage 2)

MNIST To evaluate the compression performance we use (1) a **Conv4** network consisting of 4 convolutional layers and (2) a high capacity **VGG-13** network.

Figure 3 shows the results of our compression approach for each teacher network. The lines represent the compression (blue), accuracy (green) and reward (orange). The y-axis represents the score of those quantities, between 0 and 1. The x-axis is the iteration number. We also highlight the largest and smallest models with red circles to give a sense of the magnitude of compression. This experiment appears to confirm our original expectation that the policies would improve over time.

CIFAR-10 On the CIFAR-10 dataset we ran experiments using the following teacher networks: (1) **VGG-19**, (2) **ResNet-18** and (3) **ResNet-34** networks. The experimental results are shown in Figure 4. It is interesting to note that on CIFAR-10, our learned student networks perform almost as well or better the teacher networks despite a 10x compression rate. Additionally, the models identified by our policy are smaller and perform better than those reported by Knowledge Distillation methods that use hand designed student models such as FitNets (Romero et al. 2014) (#P: 2.5M, A: 91.61%) and DDCNRNDC (Urban et al. 2016) (#P: 3M, A: 91.8%)

SVHN On the SVHN dataset, we ran experiments using **ResNet-18** network as the teacher model. We observed that the reward and compression steadily increased while the accuracy remained stable, confirming similar results to that of CIFAR-10. This is a promising indication that our approach works for a breadth of tasks and isn't dataset specific. Plots are in supplemental material.

CIFAR-100 We also verified our approach on a harder dataset, CIFAR-100 to show how our approach performs with less data per class (Figure 5). Considering the largely reduced number of parameters, the compressed network achieves reasonably high accuracy. A notable aspect of many of the final compressed models is that ReLU layers within residual blocks were removed. Another interesting result is that the compressed ResNet-34 student model outperforms the ResNet-18 model despite having fewer parameters. This can likely be explained by the increased number of residual blocks in the ResNet-34 model.

Caltech-256 The Caltech-256 experiments (supplemental material) show the performance of our approach when training data is scarce. We would like to verify that our approach does not overly compress the network by overfitting to the small number of training examples. As with the other experiments, the policies appears to learn to maximize reward over time, although the positive trend is not as pronounced due to the lack of training data. This is expected since less data means the reward signal is less robust to sources of noise, which in turn affects training of the policy.

4.4 Compression with Size Constraints

Table 2: Model Compression with Size Constraints

Model	Acc.	#Params	Compr.	Constr.
Teacher (MNIST/VGG-13)	**99.54%**	9.4M	1x	N/A
Student (Stage 1 & 2)	98.91%	**17K**	**553x**	20K
Teacher (CIFAR-10/VGG-19)	**91.3%**	38M	1x	N/A
Student (Stage 1 & 2)	90.4%	**8 62K**	**44x**	1M

While the experiments to this point used no explicit constraints, in this experiment, we add a size constraint in terms of the number of parameters via the reward function as in Section 3.3. We expect the optimization to be harder because the range of acceptable architectures is reduced.

Results are summarized in Table 2. These promising results suggest that the compression policies are able to produce sensible results despite being heavily constrained, thus demonstrating the viability of the approach in practice.

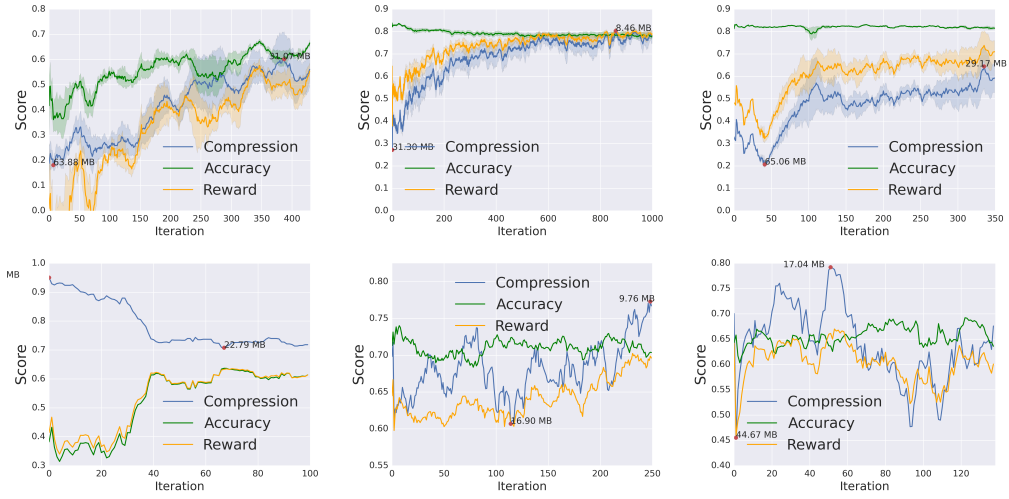

(a) VGG-19 (b) ResNet-18 (c) ResNet-34

Figure 4: Student learning on **CIFAR-10**. Reward, Accuracy, Compression vs Iteration (**Top**: Stage 1, **Bottom**: Stage 2)

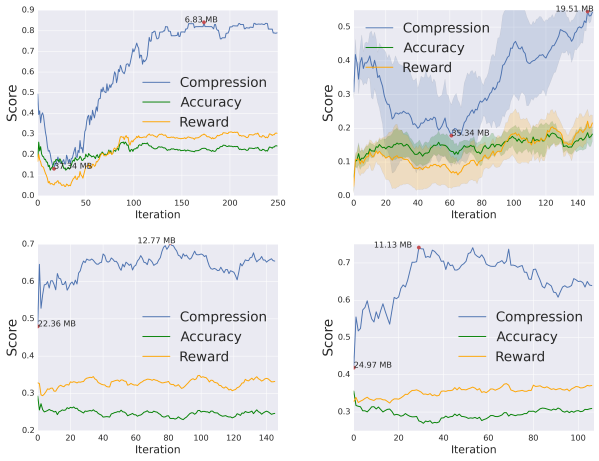

(a) ResNet-18 (b) ResNet-34

Figure 5: Student learning on **CIFAR-100**.

4.5 Transfer Learning

Naively applying our approach to a new teacher network means that the compression policies must be learned from scratch for each new problem. We would like to know if layer removal and shrinkage policy networks can be reused to accelerate compression for new teacher architectures. In the following experiments, we train a policy on an initial teacher model and then apply it to another teacher model to test whether the policy has learned a general strategy for compressing a network. Since both a pretrained policy and a randomly initialized policy will eventually converge to an optimal policy given enough iterations, we provide performance measures over the the first 10 policy update iterations.

Results are summarized in Table 3. The slight drop in accuracy (third subcolumn) in models produced by the pre-trained policy is expected due to the tradeoff between compression and accuracy. However, the average reward (first subcolumn) is always higher when we use a pretrained policy. This is an important result as it shows that we can train a policy on a *smaller* model and obtain efficiency gains on a *larger* model. This shows the potential of our approach to rapidly accelerate the policy search procedure for very deep networks, democratizing the adoption of compressed neural networks in the real world.

Table 3: Transfer Learning Performance during first 10 iterations.

	ResNet18 → ResNet34			ResNet34→ ResNet18			VGG11→ VGG19		
	Reward	Comp.	Acc.	Reward	Comp.	Acc.	Reward	Comp.	Acc.
Pre-trained	**0.81**	**78.1%**	79.5%	**0.76**	**65.5%**	82.3%	**0.52**	**46.0%**	**71.7%**
Scratch	0.50	34.8%	**82.4%**	0.53	39.7%	**82.8%**	-0.07	20.2%	42.5 %

5 Conclusion

We introduced a novel method for compressing neural networks. Our approach employs a two-stage layer removal and layer shrinkage procedure to learn how to compress large neural networks. By leveraging signals for accuracy and compression, our method efficiently learns to search the space of model architectures. We show that our method performs well over a variety of datasets and architectures. We also observe generalization capabilities of our method through transfer learning, allowing our procedure to be made even more efficient. Our method is flexible enough to incorporate other practical constraints, such as power or inference time, which hints at the diversity of future applications.

References

[Anwar, Hwang, and Sung 2015] Anwar, S.; Hwang, K.; and Sung, W. 2015. Structured pruning of deep convolutional neural networks. *arXiv preprint arXiv:1512.08571*.

[Ba and Caruana 2014] Ba, J., and Caruana, R. 2014. Do deep nets really need to be deep? In *Advances in neural information processing systems*, 2654–2662.

[Baker et al. 2016] Baker, B.; Gupta, O.; Naik, N.; and Raskar, R. 2016. Designing neural network architectures using reinforcement learning. *arXiv preprint arXiv:1611.02167*.

[Bucilu, Caruana, and Niculescu-Mizil 2006] Bucilu, C.; Caruana, R.; and Niculescu-Mizil, A. 2006. Model compression. In *Proceedings of the 12th ACM SIGKDD international conference on Knowledge discovery and data mining*, 535–541. ACM.

[Feng and Darrell 2015] Feng, J., and Darrell, T. 2015. Learning the structure of deep convolutional networks. In *Proceedings of the IEEE International Conference on Computer Vision*, 2749–2757.

[Griffin, Holub, and Perona 2007] Griffin, G.; Holub, A.; and Perona, P. 2007. Caltech-256 object category dataset.

[Guo, Yao, and Chen 2016] Guo, Y.; Yao, A.; and Chen, Y. 2016. Dynamic network surgery for efficient dnns. In *Advances In Neural Information Processing Systems*, 1379–1387.

[Han et al. 2015] Han, S.; Pool, J.; Tran, J.; and Dally, W. 2015. Learning both weights and connections for efficient neural network. In *Advances in Neural Information Processing Systems*, 1135–1143.

[Han, Mao, and Dally 2015] Han, S.; Mao, H.; and Dally, W. J. 2015. Deep compression: Compressing deep neural networks with pruning, trained quantization and huffman coding. *arXiv preprint arXiv:1510.00149*.

[Hassibi, Stork, and Wolff 1993] Hassibi, B.; Stork, D. G.; and Wolff, G. J. 1993. Optimal brain surgeon and general network pruning. In *Neural Networks, 1993., IEEE International Conference on*, 293–299. IEEE.

[Hinton, Vinyals, and Dean 2015] Hinton, G.; Vinyals, O.; and Dean, J. 2015. Distilling the knowledge in a neural network. *arXiv preprint arXiv:1503.02531*.

[Iandola et al. 2016] Iandola, F. N.; Han, S.; Moskewicz, M. W.; Ashraf, K.; Dally, W. J.; and Keutzer, K. 2016. Squeezenet: Alexnet-level accuracy with 50x fewer parameters and¡ 0.5 mb model size. *arXiv preprint arXiv:1602.07360*.

[Jozefowicz, Zaremba, and Sutskever 2015] Jozefowicz, R.; Zaremba, W.; and Sutskever, I. 2015. An empirical exploration of recurrent network architectures. In *Proceedings of the 32nd International Conference on Machine Learning (ICML-15)*, 2342–2350.

[Krizhevsky and Hinton 2009] Krizhevsky, A., and Hinton, G. 2009. Learning multiple layers of features from tiny images.

[LeCun et al. 1989] LeCun, Y.; Denker, J. S.; Solla, S. A.; Howard, R. E.; and Jackel, L. D. 1989. Optimal brain damage. In *NIPs*, volume 2, 598–605.

[LeCun, Cortes, and Burges 1998] LeCun, Y.; Cortes, C.; and Burges, C. J. 1998. The mnist database of handwritten digits.

[Ludermir, Yamazaki, and Zanchettin 2006] Ludermir, T. B.; Yamazaki, A.; and Zanchettin, C. 2006. An optimization methodology for neural network weights and architectures. *IEEE Transactions on Neural Networks* 17(6):1452–1459.

[Mariet and Sra 2015] Mariet, Z., and Sra, S. 2015. Diversity networks. *arXiv preprint arXiv:1511.05077*.

[Miikkulainen et al. 2017] Miikkulainen, R.; Liang, J.; Meyerson, E.; Rawal, A.; Fink, D.; Francon, O.; Raju, B.; Navruzyan, A.; Duffy, N.; and Hodjat, B. 2017. Evolving deep neural networks. *arXiv preprint arXiv:1703.00548*.

[Murdock et al. 2016] Murdock, C.; Li, Z.; Zhou, H.; and Duerig, T. 2016. Blockout: Dynamic model selection for hierarchical deep networks. In *Proceedings of the IEEE Conference on Computer Vision and Pattern Recognition*, 2583–2591.

[Netzer et al. 2011] Netzer, Y.; Wang, T.; Coates, A.; Bissacco, A.; Wu, B.; and Ng, A. Y. 2011. Reading digits in natural images with unsupervised feature learning. In *NIPS workshop on deep learning and unsupervised feature learning*, volume 2011, 5.

[Real et al. 2017] Real, E.; Moore, S.; Selle, A.; Saxena, S.; Suematsu, Y. L.; Le, Q.; and Kurakin, A. 2017. Large-scale evolution of image classifiers. *arXiv preprint arXiv:1703.01041*.

[Romero et al. 2014] Romero, A.; Ballas, N.; Kahou, S. E.; Chassang, A.; Gatta, C.; and Bengio, Y. 2014. Fitnets: Hints for thin deep nets. *arXiv preprint arXiv:1412.6550*.

[Saxe et al. 2011] Saxe, A.; Koh, P. W.; Chen, Z.; Bhand, M.; Suresh, B.; and Ng, A. Y. 2011. On random weights and unsupervised feature learning. In *Proceedings of the 28th international conference on machine learning (ICML-11)*, 1089–1096.

[Simonyan and Zisserman 2014] Simonyan, K., and Zisserman, A. 2014. Very deep convolutional networks for large-scale image recognition. *arXiv preprint arXiv:1409.1556*.

[Snoek et al. 2015] Snoek, J.; Rippel, O.; Swersky, K.; Kiros, R.; Satish, N.; Sundaram, N.; Patwary, M.; Prabhat, M.; and Adams, R. 2015. Scalable bayesian optimization using deep neural networks. In *International Conference on Machine Learning*, 2171–2180.

[Snoek, Larochelle, and Adams 2012] Snoek, J.; Larochelle, H.; and Adams, R. P. 2012. Practical bayesian optimization of machine learning algorithms. In *Advances in neural information processing systems*, 2951–2959.

[Srinivas and Babu 2015] Srinivas, S., and Babu, R. V. 2015. Data-free parameter pruning for deep neural networks. *arXiv preprint arXiv:1507.06149*.

[Stanley and Miikkulainen 2002] Stanley, K. O., and Miikkulainen, R. 2002. Evolving neural networks through augmenting topologies. *Evolutionary computation* 10(2):99–127.

[Urban et al. 2016] Urban, G.; Geras, K. J.; Kahou, S. E.; Aslan, O.; Wang, S.; Caruana, R.; Mohamed, A.; Philipose, M.; and Richardson, M. 2016. Do deep convolutional nets really need to be deep and convolutional? *arXiv preprint arXiv:1603.05691*.

[Warde-Farley, Rabinovich, and Anguelov 2014] Warde-Farley, D.; Rabinovich, A.; and Anguelov, D. 2014. Self-informed neural network structure learning. *arXiv preprint arXiv:1412.6563*.

[Wierstra et al. 2010] Wierstra, D.; Förster, A.; Peters, J.; and Schmidhuber, J. 2010. Recurrent policy gradients. *Logic Journal of IGPL* 18(5):620–634.

[Williams 1992] Williams, R. J. 1992. Simple statistical gradient-following algorithms for connectionist reinforcement learning. *Machine learning* 8(3-4):229–256.

[Zoph and Le 2016] Zoph, B., and Le, Q. V. 2016. Neural architecture search with reinforcement learning. *arXiv preprint arXiv:1611.01578*.

Supplemental Material

6 Actor-Critic

Policy gradient based Actor-Critic algorithms have been shown to improve the stability of the policy search. This is achieved by replacing the baseline with a learned estimate of the value function at each time step.

Formally, with vanilla REINFORCE we have,

$$\nabla_\theta J(\theta) \approx \frac{1}{m}\sum_{k=1}^{m}\sum_{t=1}^{T}[\nabla_\theta \log P_\theta(a_t|h_t)(R_k - b_k)]$$

In the Actor-Critic algorithm we replace b_k with V_k^θ, resulting in a new gradient estimate,

$$\nabla_\theta J(\theta) \approx \frac{1}{m}\sum_{k=1}^{m}\sum_{t=1}^{T}[\nabla_\theta \log P_\theta(a_t|h_t)(R_k - V_k^\theta)]$$

We implement the Critic network by adding an additional fully-connected layer that takes as input the hidden state of the LSTM and outputs a single scalar value. Below are the results of the experiments performed.

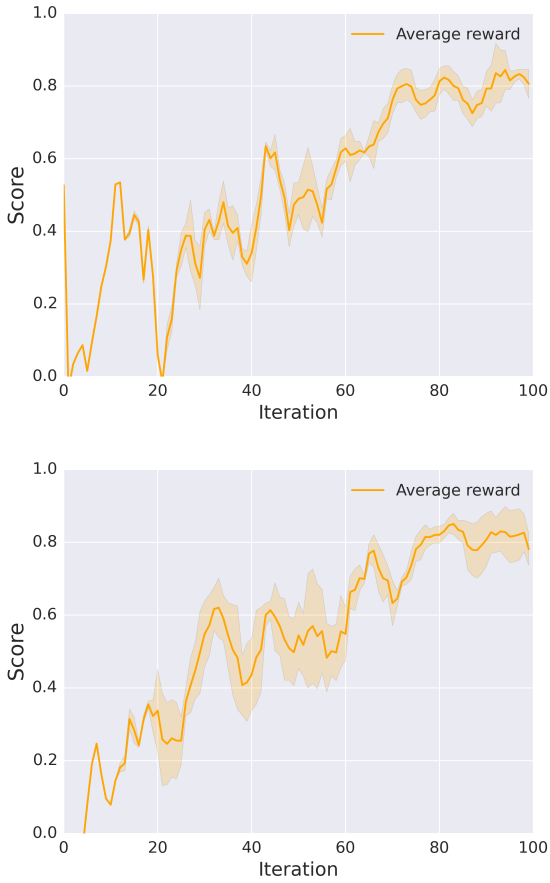

Figure 6: MNIST **Top:** Actor-critic **Bottom:** REINFORCE, averaged over 3 runs

Figure 7: CIFAR-10 **Top:** Actor-critic **Bottom:** REINFORCE, averaged over 3 runs

For the MNIST dataset, our results show that there is a slight improvement in stability, although they both converge at a similar rate.

For the CIFAR-10 dataset, although the Actor-critic version was more stable, it did not perform as well as the vanilla REINFORCE algorithm.

7 Learning rate and batch size

The learning rate and batch size were selected via a grid search. The following graphs show the rate of convergence for different learning rates and batch sizes.

7.1 Learning rate

In order to determine the learning rate, we performed a grid search over 0.03, 0.003, 0.0003. We performed this grid search on the MNIST dataset using the VGG-13 network to save time. For the stage-1 policy, it was observed that lr=0.03 did not converge while lr=0.0003 converged too slowly. Thus we used lr=0.003 as the learning rate.

Figure 8: Average reward over 3 runs for various learning rates on the MNIST dataset

7.2 Batch size

Similarly we performed a grid search to determine the optimal batch size over 1, 5, 10. A batch size of 1 was too unstable while a batch size of 10 offered no substantial improvements to justify the additional computation. Thus we observed that a batch size of 5 worked the best.

8 Transfer learning experiments

Below are the results of the transfer learning experiments, as observed, the pretrained policies start off with a high reward unlike the policies trained from scratch.

Figure 9: Average reward over 3 runs for batch sizes **Top:** 1, **Middle:** 5, **Bottom:** 10 on the MNIST dataset

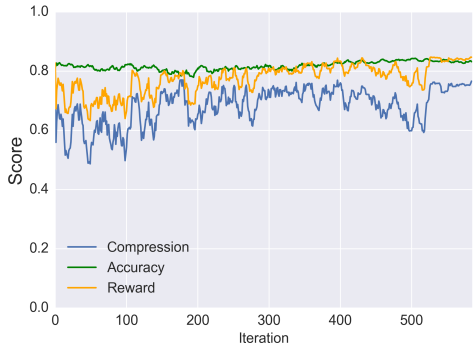

(a) ResNet18 → ResNet34

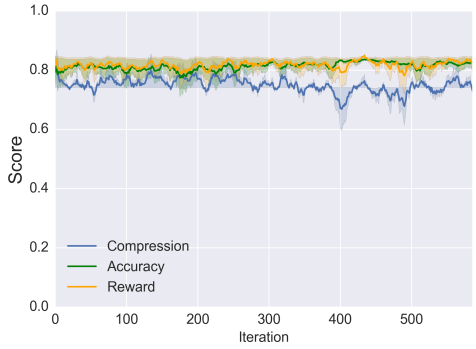

(b) ResNet34 → ResNet18

(c) VGG-11 → VGG-19

Figure 10: Transfer learning experiments

9 Additional experiments

The following section contains results about additional compression experiments that were conducted.

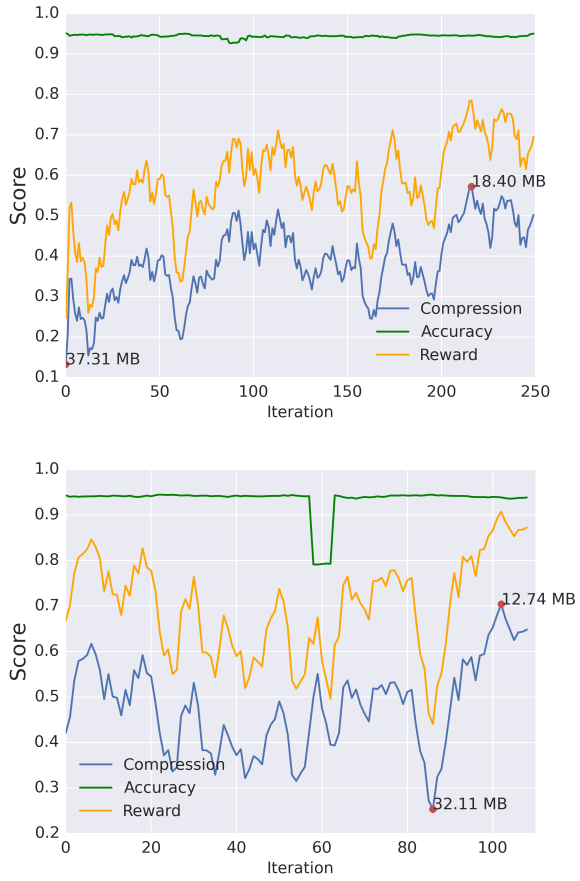

Figure 11: ResNet-18 experiments on **SVHN**, (**Top**: Stage 1, **Bottom**: Stage 2)

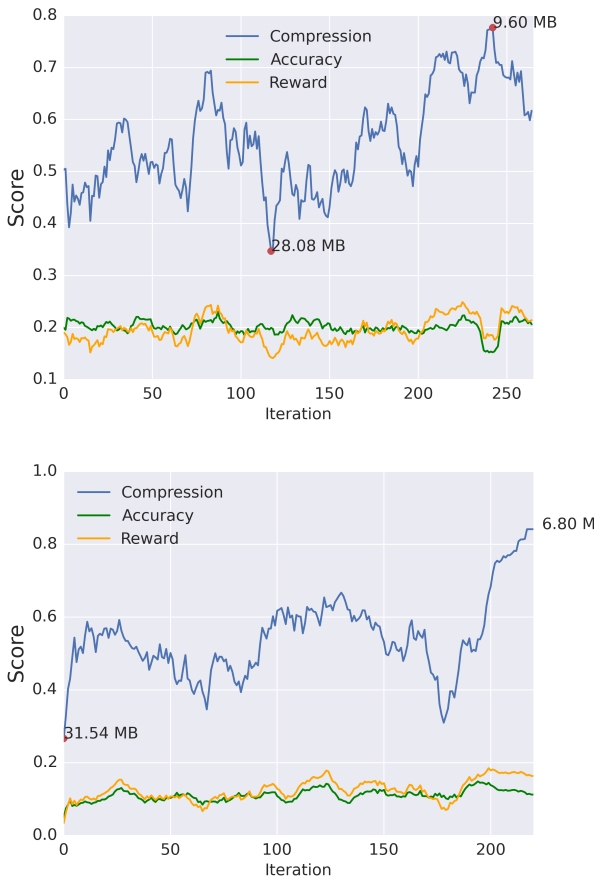

Figure 12: ResNet-18 experiments on **Caltech**, (**Top**: Stage 1, **Bottom**: Stage 2)